Abnormal physics of group-*II* telluride system: valence contribution of d electrons*

Duan He(段 鹤)[a)b)†], Dong You-Zhong(董有忠)[c)],
Huang Yan(黄 燕)[b)], and Chen Xiao-Shuang(陈效双)[b)]

[a)] *School of Physics and Optoelectronic Engineering, Guangdong University of Technology, Guangzhou* 510006, *China*
[b)] *National Laboratory for Infrared Physics, Shanghai Institute of Technical Physics, Chinese Academy of Sciences, Shanghai* 200083, *China*
[c)] *School of Physics, South China University of Technology, Guangzhou* 510640, *China*

(Received 17 October 2010; revised manuscript received 11 November 2010)

The physical trend of group-*II* tellurides is unexpected and contrary to the conventional wisdom. The present first-principles calculations give fundamental insights into the extent to which group-*II* telluride compounds present special properties upon mixing the d valence character. Our results provide explanations for the unexpected experimental observations based on the abnormal binding ordering of metal d electrons and their strong perturbation to the band edge states. The insights into the binary tellurides are useful for the study and control of the structural and chemical perturbation in their ternary alloys and heterostructures.

Keywords: group-*II* tellurides, first-principles calculations, electronic property tendency, delocalized metal d states

PACS: 31.15.E–, 71.20.–b, 81.05.Dz, 71.23.An **DOI:** 10.1088/1674-1056/20/4/043103

1. Introduction

Ternary alloys and heterostructures based on group-*II* tellurides (*II*=Zn, Cd, Hg) are currently unrivaled as leading detecting materials spanning from the infrared to the high-power spectrum.[1−5] In spite of many advantages, such as tunable band gaps, high resistivity, and excellent photosensitivity, efforts to upgrade detecting performance are hampered by the lack of control over material crystalline perfection, partly due to the structural and chemical perturbation in the ternary alloys and heterostructures, which is induced by the large size and electronic mismatch of their binary constituents.

The ternary alloys based on group-*II* telluride compounds fail to change their physical properties smoothly as a function of alloy concentration, which is different from the conventional isovalent alloys. For example, a drastic increase in the bulk modulus is found upon a small amount of Zn in CdTe,[6,7] indicating that Vegard's law cannot hold for predicting properties of such alloys as $Cd_{1-x}Zn_xTe$ with large lattice mismatch (7.4%).[8] As another example, unlike other isovalent alloys where the bonds are elongated (shortened) with the introduction of heavier (lighter) atoms into the lattice, the Hg–Te bond embedded in the CdTe lattice contracts the bond length instead and moreover the bond-lengths of Hg–Te and Cd–Te are essentially conserved in $Hg_{1-x}Cd_xTe$ relative to bulk binaries.[9,10] This reflects that it is invalid to predict the properties of group-*II* telluride binaries and their alloys in view of the argument that the added core shells completely screen the added protons along the Zn→Hg→Cd sequence. In addition, the heterostructures based on group-*II* telluride compounds also exhibit different properties from the conventional common-anion semiconductors. For instance, the CdTe/HgTe superlattice has a large valence-band offset,[11,12] which is unable to be answered from the recognized common-anion rule, predicting nearly vanishing valence-band offsets for most common-anion semiconductors. The physics of the group-*II* telluride system is fascinating but also challenging. Among the first to recognize the fascinating physics of the

*Project supported by the National Natural Science Foundation of China (Grant Nos. 10847111 and 61006091), the Startup Project for Ph. D. of Guangdong University of Technology (Grant No. 083034), and the Fundamental Research Funds for the Central Universities of South China University of Technology (Grant No. 2009ZM0022).

†Corresponding author. E-mail: duanhe@yahoo.cn

© 2011 Chinese Physical Society and IOP Publishing Ltd

group-II telluride system were Wei and Zunger,[13] who stated that the metal d electrons are indispensible for explaining the profoundly different properties of the group-II telluride system relative to the conventional isovalent alloys and common-anion semiconductors. The participation of metal d electrons in the valence band then raises a crucial question about the extent to which group-II telluride compounds present special properties upon mixing the metal d valence character in the telluride compounds, which necessitates further theoretical investigation.

In this paper, using first-principles total-energy calculations, we first study the band structures of ZnTe, CdTe, and HgTe to understand the bonding contribution of the d electrons. We find an abnormal binding energy ordering of d orbitals and the distinguishing perturbations of the metal d-state to the top-side valence states in these three telluride binaries. Then, we provide fundamental insights into the profound electronic effects of metal d electrons in these three telluride binaries, thereby providing qualitative explanations for the unexpected experimental observations in group-II tellurides.

2. Details of calculations

The present calculations used the relativistic full-potential augmented-plane-wave plus local orbitals (FLAPW+lo) method[14] in generalized gradient approximation (GGA)[15] incorporated into the WIEN2k code. The cell volume was varied isotropically and then fitted the total energy to Murnaghan's equation to obtain equilibrium lattice constants. The inner-shell electrons were distinguished from the valence electrons of metal atoms ($d^{10}5s^2$) and Te (s^2p^4) by proper separation energy. The local orbitals were introduced for metal, p and Te, d semicore states. The values of the muffin-tin radii were set differently for different systems but the same values were used for anion and cation atoms: 2.45, 2.65, and 2.64 a.u. for ZnTe, CdTe, and HgTe, respectively. $R_{\rm MT}K_{\rm max}$ was kept at 8.0. The charge density was self-consistently determined using 10×10×10 Monkhorst–Pack mesh. All of the above parameters ensured an accuracy of 0.01 mRy (1 Ry=13.605 eV) in the total energy of the systems.

3. Results and discussion

3.1. Electronic state characteristic of binary telluride

The design and analysis of ternary alloys is expected to be relevant to the features in the electronic states of their constituent binary compounds. We thus first discuss the electronic state characteristic of binary telluride. Figure 1 gives the density of states (DOS) of ZnTe together with that of CdTe and HgTe for comparison. Figure 2 is the calculated electronic structure of ZnTe. As can be seen from Figs. 1 and 2, the energy dispersion of ZnTe consists of six regions: four occupied bands (P_1–P_4) and two unoccupied ones (P_5, P_6).

The deepest valence band P_1 mostly originates from the Te 5s states, e.g., 56.7% in $\Gamma_{1\rm v}$, 67.0% in $X_{1\rm v}$, and 66.8% in $L_{1\rm v}$ for ZnTe. The charge densities in the P_1 region are localized on the Te site, as a manifestation of s orbitals atom-centred character. Since the P_1 states are atom centered, their binding energy depends on the configuration of the Te-based tetrahedron. The larger atomic-size mismatch in ZnTe and CdTe than HgTe necessitates the Te^{2-} around Zn^{2+} and Cd^{2+} to release more of the strain energy than the Te^{2-} around Hg^{2+} to adjust the bond-length freedom, and thereby the ZnTe and CdTe-related s states move to shallower binding energies (by 0.5 eV) relative to the HgTe-related s states (Fig. 1).

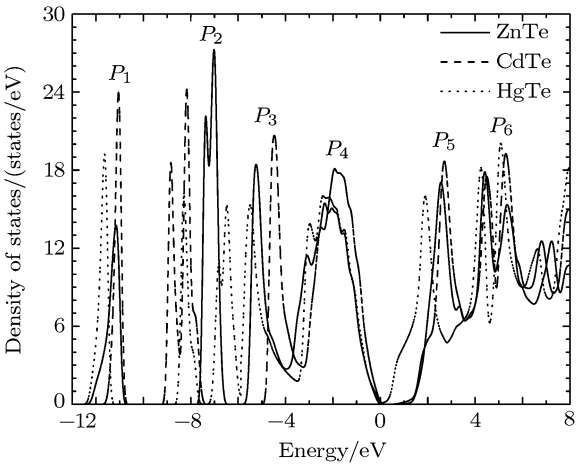


Fig. 1. Density of states (DOS) of ZnTe together with that of CdTe and HgTe for comparison. Zero of energy is at the valence band maximum (VBM).

The second deepest band P_2 has a significant metal d character, as evidenced by the charge exclusively localized on the metal sites and the exceeding 90% character ranged from the bottom-side

(Γ_{15d}) to the top-side (Γ_{12d}) of this region. Note from Fig. 3 that the Γ_{12d} state conserves the nature of the P_2 states with metal-centred localization, while the Γ_{15d} state exhibits charge buildup along the metal–Te bond, indicating admixture of bonding character into the Γ_{15d} state through strong coupling of the metal d and Te 5p states. The spin–orbit doublets ($j = 3/2$ and $5/2$) of the metal d-state is in the sequence of $d_{3/2} < d_{5/2}$. From our calculations, the energy level of the outer d orbitals decreases along the Hg→Zn→Cd sequence, and the centres of d-band energies are at −7.08, −7.10, and −8.31 eV for HgTe, ZnTe, and CdTe, respectively. In Subsection 3.2, we will further show how the different binding of metal d orbitals leads to the abnormal trend of physical properties in these three telluride compounds.

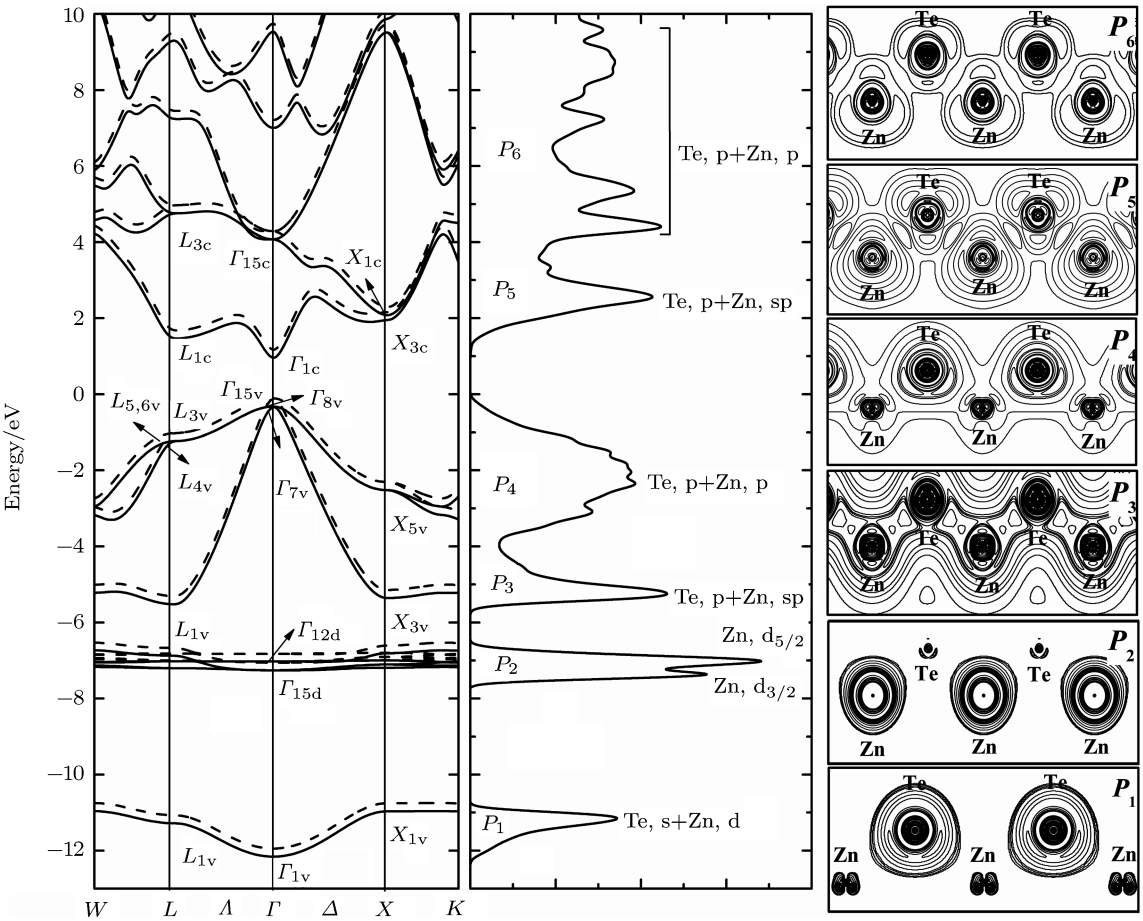


Fig. 2. Calculated band structure (solid line), density of states (DOS), and charge density associated with featured peaks (P_1–P_6) in DOS for ZnTe, as obtained using semirelativistic calculations. The nonrelativistic (dashed line) calculated band structure is also depicted.

Inspection of the orbital character in the P_3 and P_5 regions reveals an energy coincidence of the metal valence s, p states and the Te 5p states. The calculations show that the metal s orbitals have a larger energy difference than the p orbitals (e.g., −1.36, −1.43, and −1.26 eV for Zn 4p, Cd 5p, and Hg 6p states whereas −5.98 and −5.66, −7.21 eV for Zn 4s and Cd 5s, Hg 6s states, respectively), hence the energy levels of the P_3 and P_5 states for II^B–VI telluride are dominated by the order of the metal s-orbital energies. On the other hand, the P_3 and P_5 are sp^3 bond- and antibond-centered states, respectively, thus their energy levels also respond to the sp-electron overlap: the smaller metal s to Te 5p-orbital energy separation (e.g., −6.19 eV for Te 5p states) causes the shallower bond- and antibond-centred states. Therefore, CdTe has the shallowest P_3 and P_5 states while these states are deepest for HgTe.

The P_4 and P_6 regions have p-like character, e.g., the maximum of the P_4 region (Γ_{15v} state) has 53.8%

Te- and 4.9% metal-p characters for ZnTe. The Γ_{15v} state exhibits depletion of charge around the metal sites (Fig. 3) besides bonding charge buildup along the metal–Te bond, indicating that the Γ_{15v} state is not merely the extent of the metal-p character. Note that the three telluride compounds all have ∼4% metal p character in Γ_{15v} but different proportions of metal d character (8.4%, 8.0%, and 14.2% metal d character in ZnTe, CdTe, and HgTe, respectively), and the situation can be observed in the X_{1v} and L_{1v} states as well. We thus conclude that the top-side valence band of II–VI telluride is the Te and metal pp coupling with a combination of the metal d-state perturbation. It is the distinguishing contributions of the metal d-state to the top-side valence band that results in the different feature around the band edge of the three telluride compounds (see Subsection 3.2).

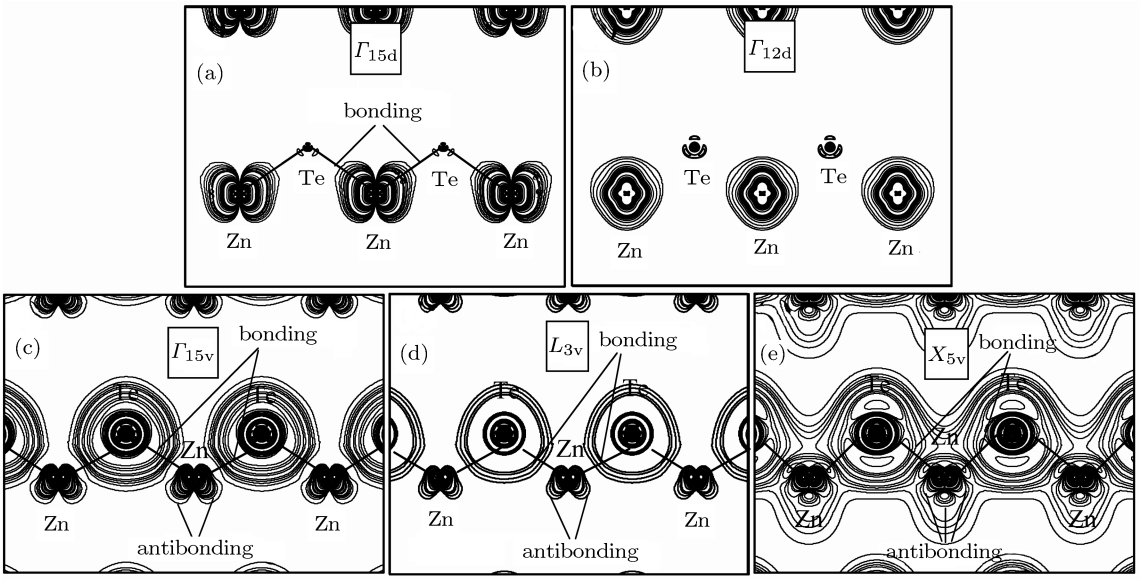


Fig. 3. Calculated charge density of the d-band states at Γ point and the top-side valence states at Γ, L, and X points for ZnTe. (a) Γ_{15d}, (b) Γ_{12d}, (c) Γ_{15v}, (d) L_{3v}, and (e) X_{5v}. Note the bonding buildup of charge along the bond in (a), the nonbonding character in (b), and the antibonding character in (c)–(e).

3.2. Abnormal trend of physical properties in binary telluride compounds

3.2.1. Lattice constants, cohesive energies, and bulk moduli

Zn, Cd, and Hg have similar s- and p-orbital energies, thus one would expect the normal trend that the compound with heavier atoms would have a larger lattice constant and cohesive energy than the compound with lighter atoms. However, experiments[1,16−19] contradict the expectations, i.e., the measured lattice constant and cohesive energy of HgTe are smaller than that of CdTe, and ZnTe has the largest cohesive energy (Table 1). This abnormal trend can be appreciated from the ordering of the binding of atomic metal-d orbitals.

Comparing nonrelativistic (NR) with semirelativistic (SR) calculations (Table 1), one can see a remarkable relativistic reduction in the lattice constant of HgTe, indicating that relativistic effects are not negligible in forming HgTe. Relativistic effects contract the Hg 6s orbitals, making them more tightly bound, which leads to (i) a reduction in the effective atomic size of Hg and subsequently, a reduction in the lattice constant of HgTe; (ii) a reduction in the direct contribution of Hg 6s electrons to the cohesive energy of HgTe; (iii) a better shield of the non-s orbitals against the nucleus, presenting Hg d electrons with a less attraction with the atomic core, so that Hg has a shallower d electrons compared with Cd and Zn, thus an enhanced antibonding repulsion between Te p and Hg d states further reduces the cohesive energy of HgTe. In this way, HgTe should have a smaller lattice constant than CdTe (which is less affected by relativistic effects) and the smallest cohesive energy among the three telluride compounds.

Table 1. Comparison of ground-state properties (lattice constant a, cohesive energy E_c, bulk modulus B) and spin–orbital splittings (Δ_0 and Δ_1 at L_{3v} and Γ_{15v} states, respectively) of group-II tellurides, obtained using nonrelativistic (NR) and semirelativistic (SR) calculations.

	ZnTe			CdTe			HgTe		
	this work		exp. [15]–[18]	this work		exp. [15]–[18]	this work		exp. [1]
property	NR	SR		NR	SR		NR	SR	
a/Å	6.146	6.101	6.089	6.559	6.483	6.480	6.831	6.660	6.461
E_c/(eV/pair)	5.08	4.79	4.82	4.80	4.53	4.45	4.89	3.99	3.22
B/GPa	54.5	49.7	50.9	43.9	43.1	44.5	41.8	46.7	47.6
Δ_0/eV		0.85	0.93		0.78	0.90		0.76	1.08
Δ_1/eV		0.50	0.57		0.51	0.57		0.54	0.62

In the case of ZnTe and CdTe, the added electron shells from Zn to Cd makes the Cd 5s wave functions penetrate not as deep as the Zn 4s wave functions, so that the Cd 5s electrons are more delocalized than that of Zn 4s electrons, presenting Cd d electrons worse screened relative to the Zn d electrons. Therefore, the increased binding of the outmost s orbitals (by 0.32 eV from Cd to Zn) leads to the decreased binding of d electrons from Cd to Zn. As the outer d electrons become shallower from Cd to Zn, they approach more closely the energies of the Te p states, causing a stronger p–d overlap interaction in ZnTe relative to CdTe. This effectively increases the contribution of the d states to the cohesive energy in ZnTe relative to CdTe. For the reasons mentioned above, the lattice constant increases along the ZnTe→HgTe→CdTe sequence (thus the bulk module follows a reverse order), and the cohesive energy increases along the HgTe→CdTe→ZnTe sequence (e.g., 3.99, 4.53, and 4.79 eV for HgTe, CdTe, and ZnTe, respectively).

3.2.2. Band edge structures

As stated above, the top-side valence band of II–VI telluride is not the extent of Te and metal pp coupling but the different proportions of metal d character. We thus believe that the distinguishing feature of their band edge structures is related to the metal d-state perturbation. For example, relativistic effects are significant in the compound with heavier atoms, so that the spin–orbit splitting is assumed to increase with the metal atomic number. However, the spin–orbit splitting Δ_1 (at L_{3v}) conserves the expectation whereas the spin–orbit splitting Δ_0 (at Γ_{15v}) follows the reverse order, i.e., Δ_0(HgTe) < Δ_0(CdTe) < Δ_0(ZnTe). The reduced Δ_0 for HgTe reflects the stronger metal d-state perturbation in HgTe relative to CdTe and ZnTe, effectively shifting the p–d antibonding state (Γ_{7v}) upwards relative to Γ_{8v} states and thus largely compensating the splitting induced by relativistic effects.

To further demonstrate the distinguishing feature of the band edge structures, we linked the first-principles calculations with the effective-mass approximation[20] to derive the effective masses for ZnTe, CdTe, and HgTe. The obtained effective electron masses (m_e^*) and the effective heavy-, light-, and spin–orbit split-off-hole masses (m_{hh}^*, m_{lh}^*, and m_{so}^*) along the [111], [100], and [110] directions are summarized in Table 2.

Table 2. Comparison of effective electron masses (m_e^*) and effective heavy-, light-, and spin–orbit split-off-hole masses (m_{hh}^*, m_{lh}^*, and m_{so}^*) of group-II tellurides. Available theoretical and experimental results are also given.

			m_{hh}^*			m_{lh}^*			
		m_e^*	[111]	[100]	[110]	[111]	[100]	[110]	m_{so}^*
ZnTe	this work	0.133	0.966	0.458	0.395	0.098	0.136	0.093	0.226
	[a]other calc.	0.135	0.960	0.419	0.365	0.102	0.136	0.098	
	[b]exp.	0.12							
CdTe	this work	0.109	1.099	0.529	0.463	0.105	0.139	0.097	0.231
	[a]other calc.	0.131	1.099	0.490	0.424	0.106	0.137	0.101	
	[b]exp.	0.095	0.69	0.6	0.35	0.21	0.18	0.131	
HgTe	this work	0.030	0.746	0.446	0.303	0.025	0.025	0.026	0.101
	[b]exp.	0.031	0.645	0.406	0.32	0.028	0.028	0.028	

[a]FLAPW method within the local density approximation from Refs. [21]–[23]. [b]Experimental values from Refs. [24]–[27].

One can see that the $m^*_{\rm hh}$ exhibits considerable k-directional dependence, while the $m^*_{\rm lh}$ shows slight anisotropy regarding different k directions and the spin–orbit split-off-hole masses are nearly isotropic. The anisotropy of heavy- and light-hole bands is relevant to the tetrahedral crystal–field splitting at the points (except for Γ), which shift the states, such as $L_{3\rm v}$ and $X_{5\rm v}$, to higher energies in different magnitudes. The isotropic spin–orbit split-off-hole band reflects a smaller perturbation of spin–orbit splitting in the upper valence band compared with that of the crystal–field splitting. Our results agree with the experimental and theoretical values,[21−27] while at the same time the abnormal effective mass ordering deserves our attention. The crystal–field splittings at L and X points act to broaden the heavy- and light-hole bands by repelling $L_{3\rm v}$ and $X_{5\rm v}$ without affecting the valence band maximum (VBM) at $\Gamma_{15\rm v}$, and to narrow the spin–orbit split-off-hole band by shifting $L_{1\rm v}$ and $X_{3\rm v}$ downwards. Hereby one expects that the compound with heavier atoms would have larger $m^*_{\rm hh}$, $m^*_{\rm lh}$ and smaller $m^*_{\rm so}$ due to more significant crystal–field splitting than the compound with lighter atoms. However, the available results fail to conserve the expectation, e.g., HgTe has smaller $m^*_{\rm hh}$, $m^*_{\rm lh}$ than CdTe and ZnTe, and CdTe has larger $m^*_{\rm so}$ than ZnTe. These can be naturally explained in terms of the upward shift of VBM through p–d mixing effects at the VBM. Since Hg d electrons are much more delocalized than ZnTe and CdTe, the p–d repulsion raises the energy of VBM so much that it contributes a considerable reduction to $m^*_{\rm hh}$ and $m^*_{\rm lh}$ of HgTe. In the same way, ZnTe has a smaller $m^*_{\rm so}$ than CdTe by enhanced p–d repulsion from CdTe to ZnTe.

4. Summary

In summary, we have studied the profound electronic effects of metal d electrons in group-II tellurides with an abnormal trend of physical properties. We found that the relativistic contraction and deep penetrability of metal s electrons alters the ordering of metal d electron binding energies. Upon mixing the metal d-electron character, the top-side valence states are shift upwards and thereby the band edge structure is alternated. The results enable us to explain a number of unexpected experimental observations, such as the abnormal trend in lattice constants, cohesive energies, and splittings induced by relativistic and crystal–field effects. The fundamental insights into the binary tellurides also provide a framework to understand and control the structural and chemical perturbation in their ternary alloys and heterostructures, which is induced by the large size and electronic mismatch of the binary constituents.

References

[1] Rogalski A 2005 *Res. Prog. Phys.* **68** 2267
[2] Berding M A 1999 *Appl. Phys. Lett.* **74** 552
[3] Berding M A, Van Schilfgaarde M, Paxton A T and Sher A 1990 *J. Vac. Sci. Technol.* A **8** 1103
[4] Wu Owen K, Rajavel R D and Jensen J E 1996 *Mater. Chem. Phys.* **43** 103
[5] Badano G, Garland J W and Sivananthan S 2003 *J. Cryst. Growth* **251** 571
[6] Ehrenreich H and Hirth J P 1985 *Appl. Phys. Lett.* **46** 668
[7] Comedi D and Kalish R 1992 *Phys. Rev.* B **46** 15844
[8] Duan H, Chen X S, Huang Y, Wang L and Lu W 2007 *Phys. Lett.* A **370** 517
[9] Sher A, Chen A B, Spicer W E and Shih C K 1985 *J. Vac. Sci. Technol.* A **3** 105
[10] Wei S H and Zunger A 1991 *Phys. Rev.* B **43** 1662
[11] Johnson N F, Hui P M and Ehrenreich H 1988 *Phys. Rev. Lett.* **61** 1993
[12] Dargys A 2008 *Phys. Stat. Sol.* B **245** 1483
[13] Wei S H and Zunger A 1988 *Phys. Rev.* B **37** 8958
[14] Blaha P, Schwarz K, Madsen G K H, Kvasnicka D, Luitz J and Karlheinz Schwarz 2001 An Augmented-Plane-Wave + Local Orbital Program for Calculating Crystal Properties (Techn. Wien, Austria) ISBN 3-9501031-1-2
[15] Perdew J P, Burke K and Ernzerhof M 1996 *Phys. Rev. Lett.* **77** 3865
[16] Qadri S B and Dinan J H 1985 *Appl. Phys. Lett.* **47** 1066
[17] Qadri S B, Skelton E F, Webb A W and Kennedy 1985 *J. Appl. Phys. Lett.* **46** 257
[18] Qadri S B, Skelton E F, Webb A W and Kennedy 1986 *J. Vac. Sci. Technol.* A **4** 1971
[19] Comedi D and Kalish R 1992 *Phys. Rev.* B **46** 15844
[20] Ramos L E, Teles L K, Scolfaro L M R, Castineira J L P, Rosa A L and Leite J R 1988 *Phys. Rev.* B **63** 165210
[21] Lawaetz P 1971 *Phys. Rev.* B **4** 3460
[22] Fei L, Hegston W E, Harrison P and Stirner T 1997 *J. Appl. Phys.* **82** 3414
[23] De Paiva R, Nogueira R A, De Oliveira C, Leite Alves H W, Alves J L A, Scolfaro L M R and Leite J R 2002 *Braz. J. Phys.* **32** 405
[24] Guldner Y, Rigaux C, Grynberg M and Mycielski A 1973 *Phys. Rev.* B **8** 3875
[25] Dang L S, Neu G and Romestain R 1982 *Solid State Commun.* **44** 1187
[26] Helm M, Knap W, Seidenbusch W, Lassnig R, Gornik E, Triboulet R and Taylor L L 1985 *Solid State Commun.* **53** 547
[27] Duan H, Chen X S, Sun L Z, Zhou X H and Lu W 2005 *Acta Phys. Sin.* **54** 5293 (in Chinese)